IL NUOVO CIMENTO VOL. 21 C, N. 5 Settembre-Ottobre 1998

On the correct surface stress for the prediction of the wind wave field and the storm surge in the Northern Adriatic Sea

P. LIONELLO(1)(*), L. ZAMPATO(1)(**), P. MALGUZZI(2)
A. TOMASIN(3)(4) and A. BERGAMASCO(4)

(1) *Università di Padova - via F. Marzolo 8, 35131 Padova, Italy*
(2) *FISBAT-CNR - via Gobetti 101, 40129 Bologna, Italy*
(3) *Università "Ca' Foscari" - Dorsoduro 3246, 30123 Venezia, Italy*
(4) *ISDGM-CNR - S. Polo 1364, 30125 Venezia, Italy*

(ricevuto il 19 Novembre 1997; revisionato il 21 Aprile 1998; approvato il 15 Maggio 1998)

Summary. — This paper discusses which formulation of the surface stress over the sea determines the most accurate prediction of the wind wave field and storm surge in the Northern Adriatic Sea. The study shows that the results of the storm surge and wind wave models, when compared to the available observations, can be used for the validation of the surface stress and of the expression adopted for the ssr (sea surface roughness). The results are representative of short fetch and young wind sea conditions. The agreement between the results and the measurements shows the feasibility of the wind wave and storm surge predictions in the Adriatic Sea and supports the dependence of the ssr, and, therefore, of the surface stress, on the spectrum of the surface wave.

PACS 92.10 – Physics of the oceans.
PACS 92.10.Hm – Surface waves, tides, and sea level.
PACS 92.10.Kp – Sea-air energy exchange processes.

1. – Introduction

This study uses the results of a storm surge model and of wave model for an indirect validation of the surface stress τ over the Adriatic Sea.

According to the common practice, in neutral stability conditions, the stress τ at the air-sea interface is derived from the surface wind speed, generally the value at ten meter level u_{10} and the drag coefficient C_{D}:

$$\tau = \rho_{\mathrm{a}} C_{\mathrm{D}} {u_{10}}^2 , \tag{1}$$

(*) E-mail: lionello@pd.infn.it
(**) Grant of the UE-MASTII project ECAWOM.

$$C_{\mathrm{D}} = \left(\frac{k}{\log(10/z_0)} \right)^2 , \tag{2}$$

where, ρ_{a} is the air density, k is the constant of von Karman, and z_0 is the roughness of surface, which, over the sea, is not constant because of the presence of the wind waves. The actual expression of the ssr (sea surface roughness) is presently controversial, and this study aims at supporting recent ideas on the dependence of the ssr on the wave spectrum.

This study seeks an indirect validation of the ssr expression by analyzing the storm surge and the wind wave field prediction in the Northern Adriatic Sea during severe Sirocco storms. Since both the surge and the wave field are forced by the field of the surface stress τ, the comparison between measurements and model prediction gives an indirect validation of it, of the momentum transfer coefficient C_{D} and of the ssr z_0.

The dependence of the ssr on the wind waves has been first described by the Charnock relation (Charnock 1955)

$$z_0 = \alpha_{\mathrm{C}} \frac{\tau}{\rho_{\mathrm{a}} g} , \tag{3}$$

where g is the acceleration of gravity, and α_{C} is the dimensionless Charnock constant which is determined empirically from large sets of open-field measurements. Wu (1982) obtained $\alpha_{\mathrm{C}} = 0.0185$([1]). Equation (3) implicitly assumes that z_0 is proportional to the swh (significant wave height) of the fully developed wind sea, which scales as $\tau/\rho_{\mathrm{a}} g$, and neglects the variations of the wave spectrum during the wave growth. Therefore, if eq. (3) is used, the dependence of the ssr on the wave spectrum is reduced to a dependence on the surface wind speed. Hereafter, the ssr, C_{D} , and τ computed on the basis of eq. (3) will be referred to as "wind-dependent" quantities.

In the last few years new expressions that include an explicit dependence of z_0 on the wave spectrum have been proposed. For a pure wind sea, both experiments and theoretical models suggest that z_0 should decrease for increasing wave age α_{10} defined as $\alpha_{10} = C_{\mathrm{p}}/u_{10}$, where C_{p} is the phase velocity of the frequency at the peak of the wave spectrum. The wave age increases because the phase velocity, C_{p}, increases progressively during the wave growth. For an old wind sea α_{10} is approximately 1 or larger, while it has a smaller value for a young wind sea.

The available experimental evidences have been reanalyzed in the literature (Donelan *et al.*, 1993, Komen *et al.* 1996). Donelan *et al.* (1993) fit the available open-field measurements with the law

$$z_0 = 6.7 \cdot 10^{-4} \sigma \alpha_{10}^{2.6} , \tag{4}$$

where σ is the rms wave height. The theories that describe the effect of the waves on the ssr are based on the wave-induced stress that is associated to the wave-coherent fluctuations produced by the wind waves in the air flow (Janssen 1989, Janssen 1991, Makin *et al.*, 1995). In these studies, the vertical structure of the stress in the neutral boundary layer, where $\frac{\partial}{\partial z}\tau = 0$, has been resolved with the condition $\tau = \tau_{\mathrm{aw}} + \tau_\nu + \tau_t$. The overall stress results from the superposition of the turbulent stress τ_{t}, the viscous stress τ_ν, and

([1]) Other values have been proposed, *e.g.*, the BOLAM model used in this study for computing the surface wind field and the sea level pressure adopts $\alpha_{\mathrm{C}} = 0.032$.

the wave-induced stress τ_{aw}. The τ_{aw} contribution is specified from the wind input source function S_{in}:

$$\tau_{\mathrm{aw}} = \rho_{\mathrm{w}} \int f S_{\mathrm{in}} \cos(\theta - \theta_{\mathrm{W}}) \mathrm{d}f \mathrm{d}\theta \,, \tag{5}$$

where ρ_{w} is the water density, f is the wave frequency, θ is the direction of wave propagation, and θ_{W} is the wind direction. Janssen obtains

$$z_0 = \frac{\hat{\alpha}_{\mathrm{C}} \tau}{g\sqrt{1 - \tau_{\mathrm{aw}}/\tau}} \,, \tag{6}$$

where $\hat{\alpha}_{\mathrm{C}} = 0.0144$ is a "reduced" Charnock's constant. Makin obtains

$$z_0 = \frac{0.14\nu}{\sqrt{\tau - \tau_{\mathrm{aw}}}} \,, \tag{7}$$

where ν is the air viscosity. A "large" variation of the energy of the short waves during the development of the wave spectrum would, consequently, produce a large variation of τ_{aw} (Janssen 1989, Janssen 1991).

Both Janssen's and Donelan's formulas determine a similar decrease of z_0 during the wave growth, with Janssen's theory suggesting a slightly higher value in a young sea. This variation of z_0 with the wave age means that the Charnok parameter α_{C} in eq. (3) is not actually a constant. When the sea is young ($\alpha_{10} \approx 0.5$) both Janssen's and Donelan's formulas are approximately equivalent to eq. (3) with $\alpha_{\mathrm{C}} = 0.032$. In fact, this high value has already been used to reproduce the increase of the ssr due to the waves (Mastenbroek *et al.* 1993). When the sea is old ($\alpha_{10} \approx 1.0$) both formulas give a smaller roughness than eq. (3) with $\alpha_{\mathrm{C}} = 0.0185$, which was found the best fit to a large set of available data (Wu 1982), and can be considered the average over different values of the wave age. Janssen's theory will be used in this study and z_0, C_{D}, and τ computed on its basis will be referred to as "wave dependent".

Because of the large scatter in the measurements and the assumptions used in the theories, this dependence of the ssr on the waves remains an open issue that requires further investigations. The aim of this study is the indirect validation of this dependence by using the surface stress to force a storm surge and a wave model and by comparing the model results with sea level and ocean wave measurements. This validation, though indirect, is effective since the accuracy of the surface stress, which is the common forcing of the storm surge and the ocean wave model, is the main factor responsible for the accuracy of the models results in the Adriatic Sea.

The Adriatic Sea is a good test case for the study of the surface stress dependence on the wave field, because, during an intense Sirocco storm, the waves are far from a fully developed state. Typically, during an intense storm, when the wind is blowing along the main axis of the basin, the wave characteristics are: significant wave height swh $= 3$ m, peak period $T_{\mathrm{p}} = 9$ s, wind speed at the 10 m level $u_{10} = 20$ m/s, giving for the wave age the value $\alpha_{10} = 0.75$, which is characteristic of a wind sea in the middle stage of its growth. When the wind direction turns to the left in the Northern part of the Adriatic, then a younger wind sea reaches the northern coast. The measurements of wind, surge, and waves, unfortunately available simultaneously only at one station, are taken at the CNR Platform "Acqua Alta" located in a very convenient position (see fig. 1), where the

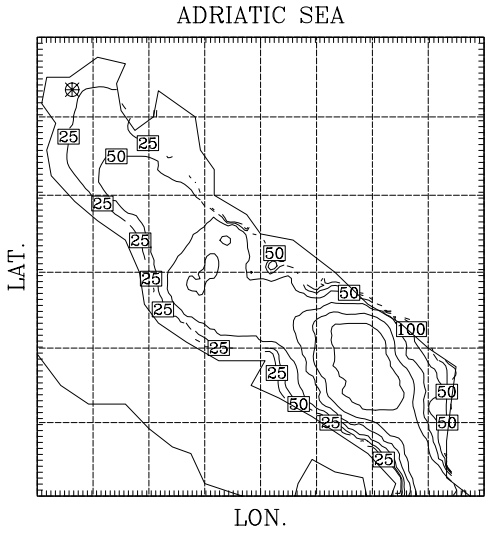

Fig. 1. – The bathymetry of the Adriatic Sea. The symbol shows the location of the platform "Acqua Alta" where the measurements have been taken.

surge is close to its maximum level, water is not particularly shallow (the depth at the station is 15 m), and there is no shadowing due to coastal features of nearby islands.

The quality of the surface stress is the main factor that conditions the results of a surge model in the Northern Adriatic Sea, while the sea level pressure is responsible approximately only for 10% of the overall surge([2]). The sea level at the open southern boundary is kept almost constant for the duration of a storm by the presence of the deep Ionian Sea acting as an infinite reservoir of water. The level of the Ionian sea can actually vary, mainly because of variations of the sea level pressure, and this is a source of error, of the order of few centimeters, that is not accounted for in this study([3]). The presence of seiches generated by previous storms and, more generally, the determination of the initial condition is a major problem for operational prediction, that can be easily avoided in the analysis of selected hindcast cases, by identifying the seiche in the measurements and by linearly superimposing it to the model results. In any case, there was no evidence of any relevant preexisting seiche in the hindcast cases presented in this paper, and their simulation was initiated approximately 3 days before the peak of the storm in order to allow the spin-up of the surge model.

The quality of the surface stress is also responsible for the results of the wave model. The swell, eventually travelling across the Otranto Strait, is likely to follow a path leading to the Eastern coast of the Southern Adriatic Sea and it does not influence the sea state in the northern part of the basin, unless for a possible minor and indirect effect on the initial growth of the wind sea in the southern part of the Adriatic. In this study, the initial

([2]) The overall surge is typically 1 m, while the difference between the value of the sea level pressure in the North and in the South of the basin, that is typically 10 hPa, produces approximately a 10 cm surge.

([3]) This is not expected to be a significant source of error. Note that the average level in the 10 days before the beginning of the simulation is taken as the reference zero level in this study.

date of the hindcast has been chosen approximately 3 days before the peak of the storm, while the spin-up time of the wave model is approximately 1.5 days. Hence, there is no influence of the initial condition on the simulation of the wave field during the main part of the storm.

The computation of the stress needed for wave and surge prediction in the Adriatic Sea is affected by two sources of uncertainty: the surface wind speed u_{10} and the ssr used for the computation of the momentum transfer coefficient C_{D}. The direct validation of the surface wind field is difficult because it has to be carried out using data usually located at coastal stations, that are often drastically affected by the local orographic features of the high mountain ridges surrounding the basin. Very few time series of *in situ* data are available over the sea, and satellite data have, up to now, not been able to provide a regular coverage of this narrow basin. This study intercompares the results obtained by using "wave-dependent" and "wind-dependent" ssr in order to investigate the effect on the storm surge and wave prediction and determine the more reliable expression in the conditions typical of the Adriatic Sea. This study, partially, rianalyses the conclusions of a previous work (Mastenbroek *et al.*, 1993), in which the storm surge in the North Sea was analyzed, and shows that the parallel simulation of the wave field and storm surge, and the comparison with *in situ* observations can be an effective tool for the assessment of the validity of different formulations of the ssr.

The paper consists of 4 sections. Section **2** is split into two parts: a description of the numerical models used and a description of the evolution of the storms analysed in this study. Section **3** analyses the results of the simulations and discusses the importance of the effect of the wave-dependent ssr for the prediction of surge and waves in the Northern Adriatic Sea. Section **4** summarizes the main conclusions of the study.

2. – The numerical simulation of the storms

Four storms have been selected. They are representative of intense cases of surge and high wave conditions in the Northern Adriatic. The selected cases took place in late autumn, which is the usual time of the year for high surge and wave events in the basin. For all cases wind, wave and sea level measurements taken at the CNR research platform "Acqua Alta" are available. The simulations are based on the use of three models: the atmospheric circulation model BOLAM (Bologna Limited Area Model), the wave model WAM (WAve Model) and the barotropic model of the marine circulation provided by the so-called "external" mode of POM (Princeton Ocean Model). The results of BOLAM are used for forcing both WAM and POM, but the analysis of its results from the meteorological point of view is outside the scope of this paper.

2'1. *The models.* – The output of the atmospheric models used for this study are the sea-level pressure (needed for the computation of the surge) and the wind speed at the 10 m level (needed for the computation of both the surge and the wave field). These meteorological fields have been provided by BOLAM, developed at FISBAT (Buzzi *et al.*, 1992). The BOLAM is a grid point, hydrostatic model in sigma coordinates, computing zonal and meridional wind components u, v, potential temperature, specific humidity and surface pressure. The physics of the model includes the parameterization of the vertical diffusion depending on the Richardson number, dry adiabatic adjustment, the soil water and energy balance (the sea surface temperature is prescribed), radiation, the effect of clouds, large-scale precipitation, condensation, evaporation, and moist convection. The adopted grid step is 0.20 degrees in latitude and 0.25 degrees in longitude.

The wave field has been computed using WAM. WAM (WAMDI Group 1988) solves the energy transfer equation:

$$\frac{\partial F(f,\theta,\bar{x},t)}{\partial t} + \nabla(c_{\rm g} F(f,\theta,\bar{x},t)) = S_{\rm in} + S_{\rm nl} + S_{\rm ds} + S_{\rm bf}, \tag{8}$$

describing the variation of the wave spectrum F in space $\bar{x}$ and time t due to the advection of energy and to the local interactions. Here f is the wave frequency, θ the wave direction and $c_{\rm g}$ the group velocity. The wave spectrum is locally modified by the input of energy from the wind, the redistribution of energy due to the nonlinear interactions, the energy dissipation due to wave breaking, and the bottom friction. These processes are represented by the source functions $S_{\rm in}$, $S_{\rm nl}$, $S_{\rm ds}$, and $S_{\rm bf}$, respectively. A detailed description of the model is given in the original paper (WAMDI 1988). The resolution adopted has been $1/6$ degrees. WAM contains a scheme for the computation of a wave age-dependent momentum transfer coefficient computed on the basis of Janssen's theory from an iterative solution of eqs. (1),(2), (6), and (5). Therefore, in the simulations contained in this section, the wave field is computed accounting for the effect of the waves on the surface stress.

The sse (sea surface elevation) has been computed using a nonlinear barotropic shallow-water model. This model has been extracted from POM (Blumberg and Mellor, 1987) and it corresponds to its so-called "external mode", with only minor modifications, mainly the insertion of the extra forcing due to the atmospheric sea level pressure, without changing the model numerics. The model computes the sse η, and the (vertical) average of the horizontal velocity $\bar{U}$:

$$D\bar{U} = D(U,V) = \int_{-H}^{\eta} (u,v)\mathrm{d}z = \int_{-H}^{\eta} \bar{u}\mathrm{d}z\ , \tag{9}$$

where H is the water depth and $D = H + \eta$ the total depth of the fluid. The model equations are derived from the vertical average of the momentum equation assuming a constant velocity profile:

$$\begin{aligned} \frac{\partial DU}{\partial t} + \nabla D\bar{U}U &= -gD\frac{\partial}{\partial x}(\eta + \frac{p_{\rm a}}{\rho_{\rm w} g}) + f_{\rm C} DV + \frac{\tau_{x{\rm a}} - \tau_{x{\rm b}}}{\rho_{\rm w}} - \nabla\bar{\Gamma}_x\ , \\ \frac{\partial V}{\partial t} + \nabla D\bar{U}V &= -gD\frac{\partial}{\partial y}(\eta + \frac{p_{\rm a}}{\rho_{\rm w} g}) - f_C DU + \frac{\tau_{y{\rm a}} - \tau_{y{\rm b}}}{\rho_{\rm w}} - \nabla\bar{\Gamma}_y \end{aligned} \tag{10}$$

and the continuity equation

$$\frac{\partial \eta}{\partial t} = -(\frac{\partial DU}{\partial x} + \frac{\partial DV}{\partial y}) = -\nabla D\bar{U}\ . \tag{11}$$

Here ∇ is the horizontal divergence, $\bar{v} = (u,v)$ is the current speed, $\bar{\Gamma}_x$, $\bar{\Gamma}_y$ represent the momentum fluxes due to subgrid features, described using the Smagorinsky diffusivity, $\tau = (\tau_{x{\rm a}}, \tau_{y{\rm a}})$ and $\tau_{\rm b} = (\tau_{x{\rm b}}, \tau_{y{\rm b}})$ are the surface and the bottom stress, respectively,

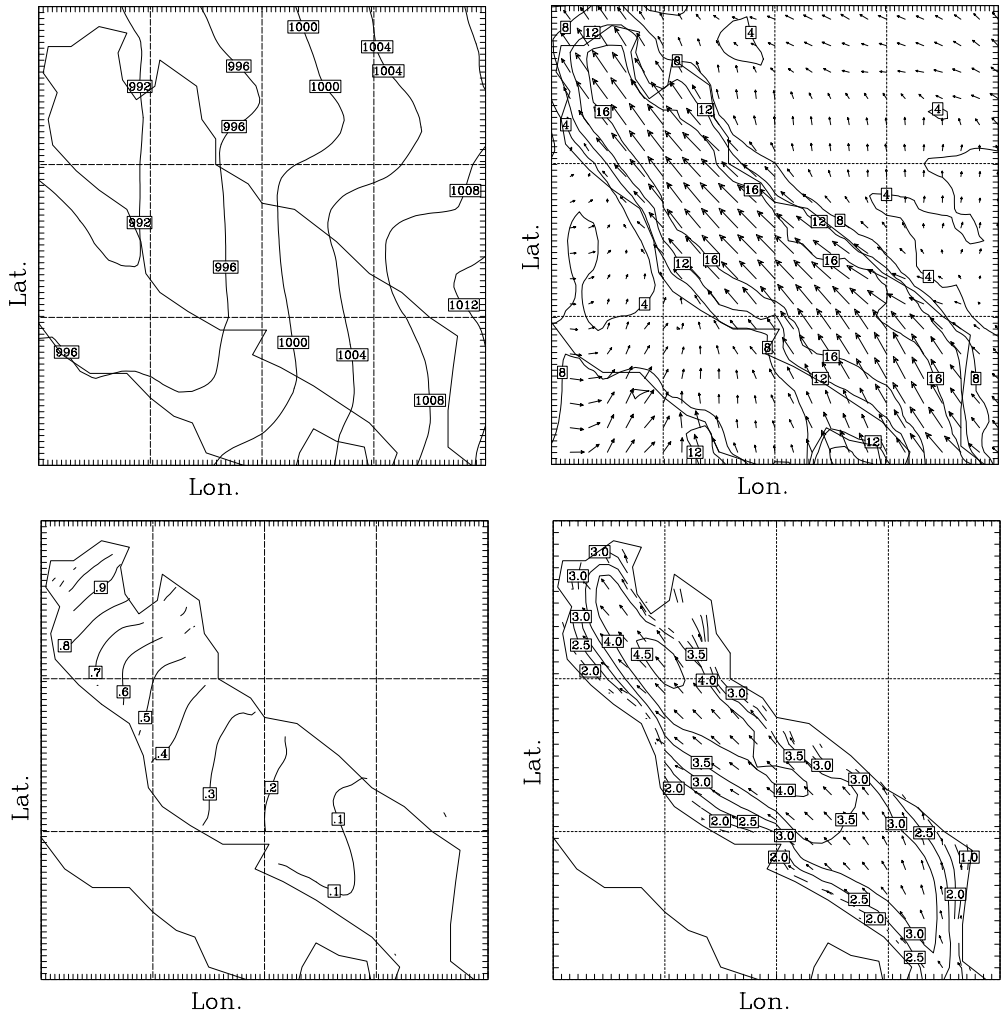

Fig. 2. – Computed fields on 10th Dec. 1990 at 3 UT. Top-left panel: Sea level pressure (contours every 4 hPa). Top-right panel: wind speed at 10 m (contours every 4 m/s). Bottom-left panel: sea level (contours every 10 cm). Bottom-right panel: significant wave height (contours every 0.5 m).

p_{a} is the atmospheric pressure, and f_{C} the Coriolis parameter. The bottom stress is represented by a quadratic friction law with a drag coefficient $C_{\mathrm{b}} = 0.0025$. The grid step is 1/12 degrees.

The motion of the ocean is externally forced by the wind stress and the atmospheric pressure. The atmospheric pressure and the wind at 10 meter level are directly supplied by the BOLAM atmospheric circulation model and they are linearly interpolated at the higher resolution of the wave and surge models. The wind stress is derived from the 10 meters using the momentum transfer coefficient C_{D}, computed by WAM.

2˙2. *Description of the hindcast cases.* – The four hindcast cases simulated here are named 87112112, 90112212, 90120700, 91112312 after the initial time of the simulation

of each event, specified in the format YYMMDDHH (YY = year, MM = month, DD = day, HH = hour).

The evolution of the first three cases is rather similar. They represent typical Sirocco storms, produced by a low pressure centered over Northern Italy or the Ligurian Sea which produces a strong cyclonic circulation. The low-pressure system moves in the Mediterranean Sea from the West, getting intensified by the combined action of the orography and of the sea surface temperature, which is warmer than the air coming from continental Europe. The wind over the Adriatic is intensified by the channeling between the Dinaric Alps and the Apennines. The maximum speed, located on the eastern side of the Northern Adriatic, has a value between 15 m/s and 25 m/s. The wind sea is generated by the Sirocco wind in the southern deep part of the basin, it continues growing in the

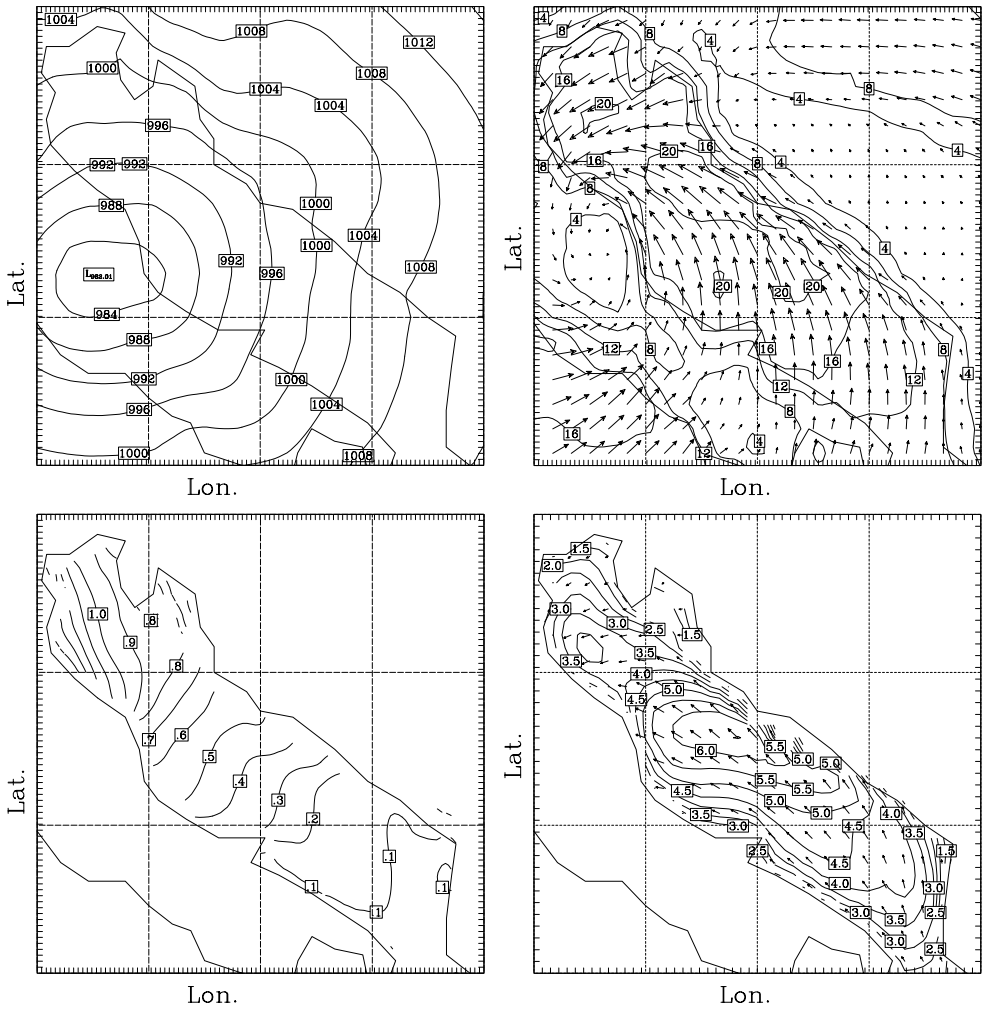

Fig. 3. – Computed fields on 24 Nov. 1991 at 15 Ut. Top-left panel: Sea level pressure (contours every 4 hPa). Top-right panel: wind speed at 10 m (contours every 4 m/s). Bottom-left panel: sea level (contours every 10 cm). Bottom-right panel: significant wave height (contours every 0.5 m).

central part, and it reaches the maximum height in the central and northern parts, where the swh can be larger than 4 m. The combined action of the wind stress and atmospheric pressure gradient enhances the sea level in the northern shallow part, sometimes reaching an almost steady state where the gradient of the sea level balances the surface stress and compensates for the variation of the atmospheric pressure. During a strong surge event, the increase of the sea level in the shallow Northern area, where the water depth is in the range 10–30 m, reaches approximately 1 m. Figure 2 shows the fields at the most intense phase of the 90120700 storm.

The development of the 91112312 storm was different. An intense cyclone originated over North Africa, precisely over Libya, became extremely intense while crossing the Sicily Channel, and it continued, with progressively decreasing strength, in the North-East direction, reaching the northern part of the Adriatic Sea, where the wind associated with the low pressure, centered in the middle of the Adriatic Sea, during the second part of the storm, was channeled and intensified by the surrounding mountains ridges. The pattern of both the waves and surge distributions is more complicated in this case than in the previous ones, because in the central part of the basin the wind is blowing along its axis, while in the northern part it becomes north-easterly, blowing almost parallel to the Venetian coast, with a fetch much shorter than in the other cases. The mean wave direction is turned toward South-West, producing a slanting fetch growth and a wave field very sensitive to the details of the coastline. The pattern of the sea level in the Adriatic is a consequence of the pattern of the wind field. The water is pushed towards the North in the central and southern part of the Adriatic and towards the western coast in the northern part. Therefore, the sea level gradient follows the main axis of the basin in its central part and it turns towards West in the Northern shallow part. Figure 3 shows the fields at the most intense phase of the 91112312 storm.

3. – A discussion on the correct computation of the sea surface roughness

Each hindcast case has been simulated twice, using the two alternative formulations, in order to investigate whether the adoption of Janssen's wave-dependent ssr of eq. (6) gives better results with respect to the wind-dependent Charnock formula of eq. (3).

Actually, instead of the Charnock formula, a drag coefficient linearly depending on the wind speed u_{10} has been used:

$$C_{\mathrm{D}} = A + B u_{10}, \tag{12}$$

where $A = 0.49 \cdot 10^{-3}$and $B = 0.065 \cdot 10^{-3}$ s/m if $u_{10} > 11$ m/s, and $A = 1.2 \cdot 10^{-3}$ and $B = 0$ otherwise (Large and Pond, 1981). This type of expression for C_{D} has been proved to be numerically equivalent to the Charnock formula for ssr (Wu 1982). These values of A and B have been obtained by a best fit to a large data set of open field observations and they can be considered to represent an average over the wind wave age.

Figures 4-7 show the results of the model simulations and the observations for the four hindcast cases at the CNR platform "Acqua Alta". In each figure, the panels (from top to bottom) show the time series of the wind u_{10}(upper panel), the square friction velocity $u_*^2 = \tau/\rho_{\mathrm{a}}$, the sse, and the swh. The line denoted with circles show the observations, the continuous line the results obtained using Janssen's (wave-dependent) formulation for the ssr and the dashed line the results obtained using the linear (wind-dependent) expression for C_{D} of eq. (12).

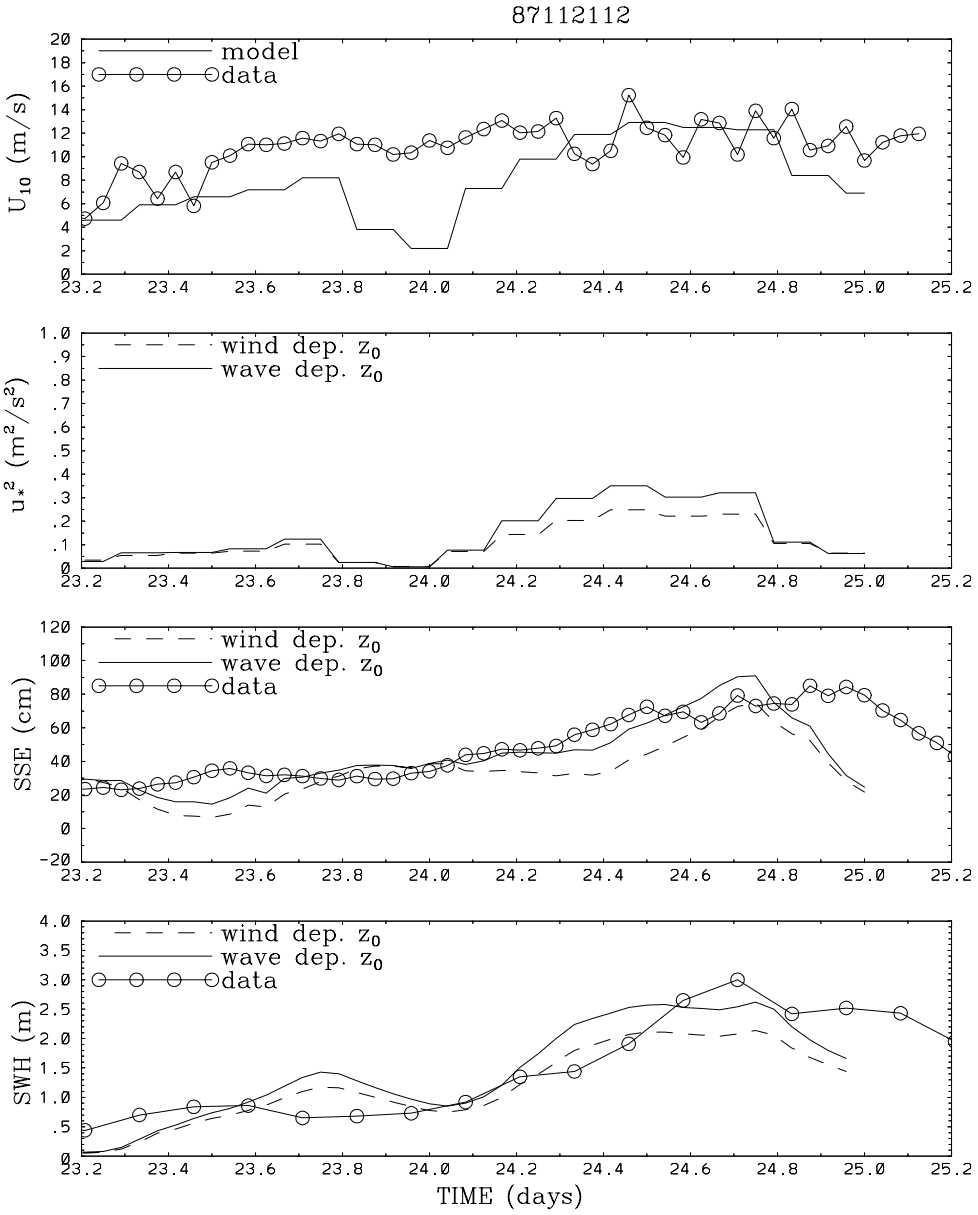

Fig. 4. – Time series for the hindcast 87112112 at the CNR platform "Acqua Alta". From top to bottom: wind at the 10 m level, squared friction velocity, sse, swh. The continuous line and the dashed line show the results of the simulation where, respectively, the wave-dependent and the wind-dependent ssr have been used, the line annotated with circles shows the observations.

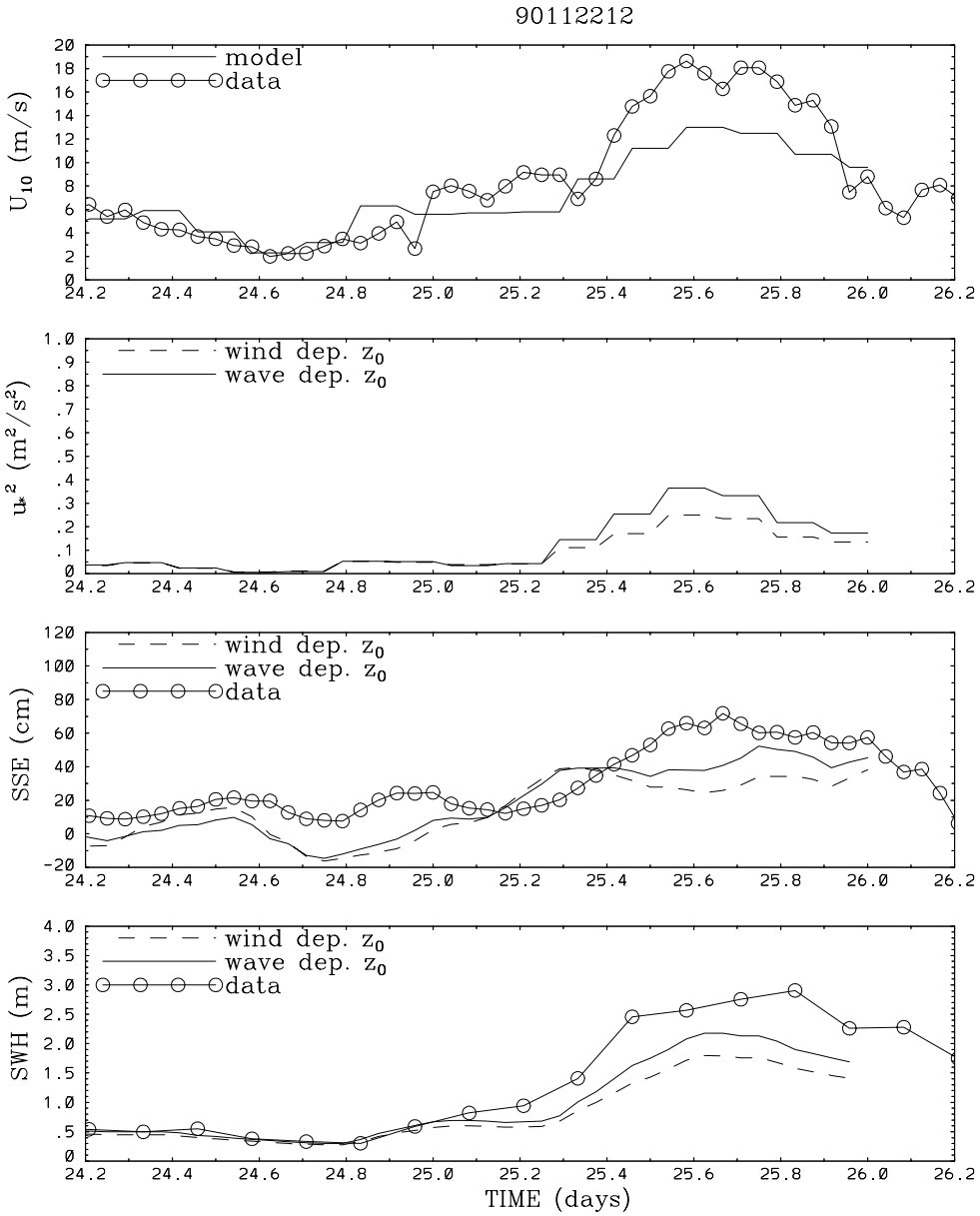

Fig. 5. – Time series for the hindcast 90112212 at the CNR platform “Acqua Alta”. From top to bottom: wind at the 10 m level, squared friction velocity, sse, swh. The continuous line and the dashed line show the results of the simulation where, respectively, the wave-dependent and the wind-dependent ssr have been used, the line annotated with circles shows the observations.

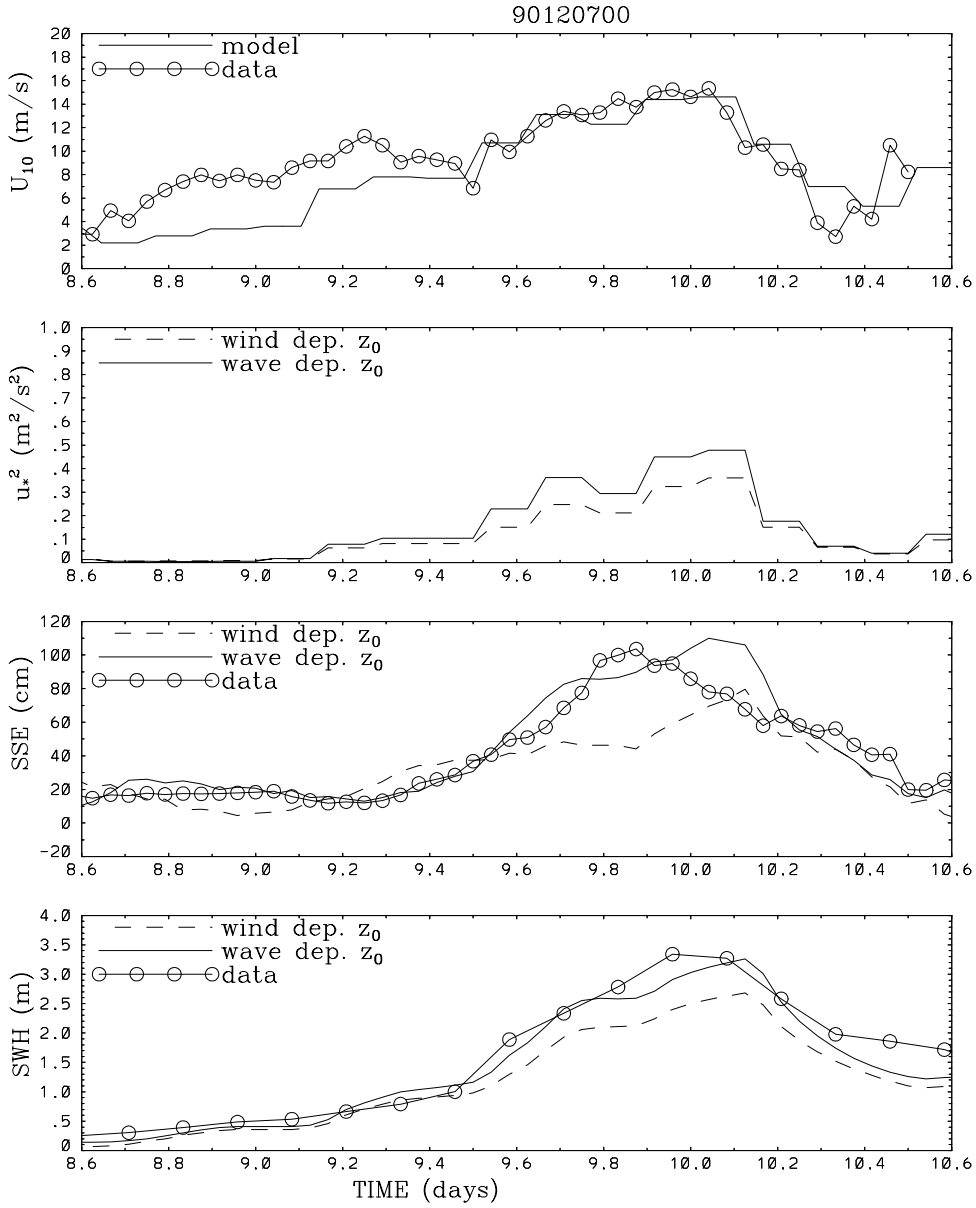

Fig. 6. – Time series for the hindcast 90120700 at the CNR platform “Acqua Alta”. From top to bottom: wind at the 10 m level, squared friction velocity, sse, swh. The continuous line and the dashed line show the results of the simulation where, respectively, the wave-dependent and the wind-dependent ssr have been used, the line annotated with circles shows the observations.

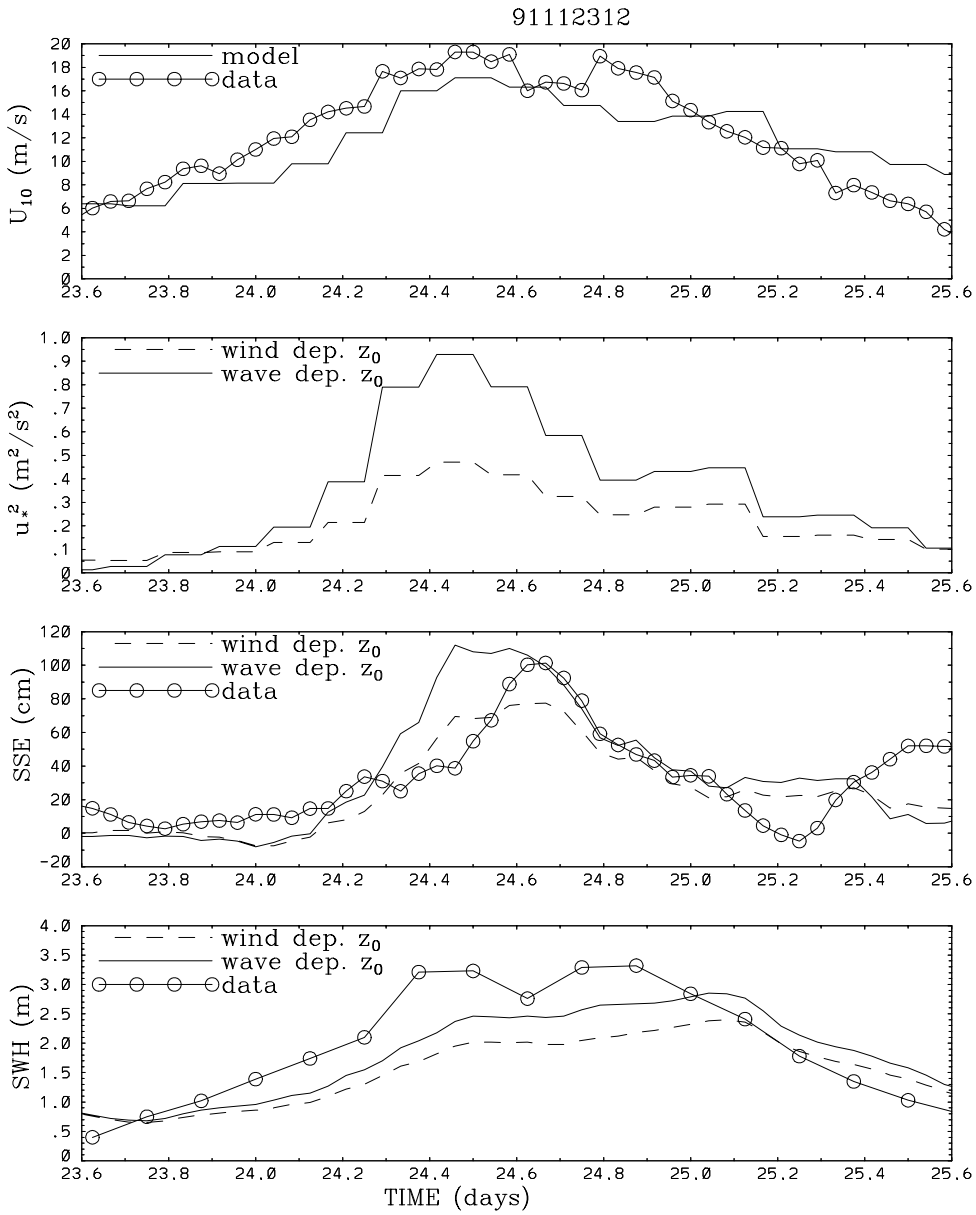

Fig. 7. – Time series for the hindcast 91112312 at the CNR platform "Acqua Alta". From top to bottom: wind at the 10 m level, squared friction velocity, sse, swh. The continuous line and the dashed line show the results of the simulation where, respectively, the wave-dependent and the wind-dependent ssr have been used, the line annotated with circles shows the observations.

The results produced using the wave-dependent ssr are generally more accurate and they reproduce better the observed behaviour of the swh and the sse. In most cases, the wave-dependent ssr eliminates the underprediction that is present when eq. (12) is used. However, the wave-dependent ssr cannot compensate for the severe underprediction of storm 90112212, which is clearly due to the underprediction of the wind speed (fig. 5). On the other hand, during the first part of storm 91112312, the wave-dependent ssr resulted in a large overprediction of the sea level suggesting an overestimation of the ssr . Note that, on the contrary, in this storm, the swh was underpredicted. Likely, this is not related to an uncorrect forcing, but to the difficulty of properly resolving the details of the wave field in the vicinity of the coast during a slanting fetch growth, and, possibly, to some problems in the numerics of the energy advection term. In fact, during the most intense part of this storm, the wind was blowing parallel to the shoreline of the Northern Adriatic.

The use of the two different formulations eq. (3) and eq. (6) has an appreciable effect on both the sse and the swh field. During the storm, the "wave-dependent" ssr produces both higher sse and swh than the "wind-dependent" formulation. The effect of the two different formulations is approximately proportional to the difference between the respective forcing surface stress fields on both sse and swh because, in steady conditions, both the sse and swh are proportional to the stress. Note, however, that, during the two most intense storms (90120700 and 91112312) the surge model is slightly more sensitive to difference in the surface stress formulation than the wave model because of its faster response time to short intense events. The sse increase is transported by the long shallow-water gravity wave with a group velocity $C_{\mathrm{S}} = (gH)^{1/2} \approx 20$ m/s, where g is the gravity acceleration and $H \approx 40$ m is the water depth. Since the main rise of the sea level takes place in the shallow part of the Northern Adriatic Sea with an effective fetch $L \approx 200$ km, the resulting response time $T_{\mathrm{s}} = L/C_{\mathrm{s}}$ is a couple of hours. The growth time of swh is proportional to the friction velocity $u_* = (\tau/\rho_{\mathrm{a}})^{1/2}$, and for an intense Sirocco storm in the Northern Adriatic Sea is approximately 0.75 day. The difference between "wind-dependent" and "wave-dependent" surface stress is large only during the intense part of the storm and the shorter response time of the surge determines its higher sensitivity.

The results of the wave model are affected by the variation of the surface stress because the source function S_{in} depends on the friction velocity:

$$S_{\mathrm{in}} = \gamma F \ , \ \gamma = \sigma \epsilon \frac{\beta_{\mathrm{m}}}{k^2} \mu \log \mu \left(\frac{u_* \cos(\theta_{\mathrm{W}})}{C_{\mathrm{ph}}} \right)^2 \ , \tag{13}$$

where $\beta_{\mathrm{m}} = 1.2$, σ is the circular frequency, k is von Karman's constant and μ is the dimensionless critical height: $\mu = kz_{\mathrm{c}}$ (z_{c} is the height where the wind speed is equal to the friction velocity). The increase in friction velocity due to the effect of the waves on the ssr gives a better reproduction of the observed swh and suggests that the wave-dependent ssr allows a more accurate value of the wind stress over sea. However, the rate of growth of the wave energy results from the difference between wind input, S_{in} and dissipation S_{ds}. The rate of energy transfer from the wind S_{in} to the wave is very difficult to assess independently of the rate of dissipation S_{ds}. The expression of S_{ds} itself is not well known and the one adopted in WAM comes from heuristic arguments and the need of a closure for the energy balance eq. (8). Therefore, even though the parameters involved in S_{in} and S_{ds} are fixed by a best fit of a large set of observed data describing the evolution of the wave spectrum, there is doubt whether the increase of S_{in} is real or is required for compensating an overestimation of S_{ds}.

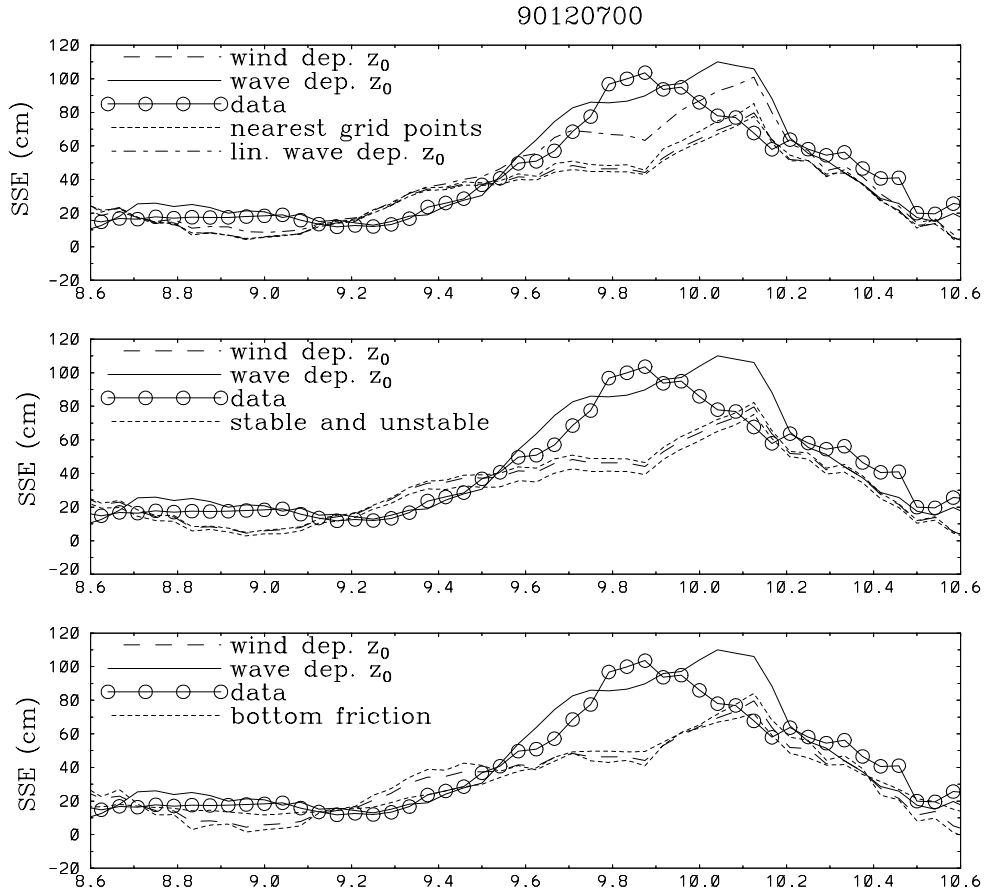

Fig. 8. – Time series of the sse at the "Acqua Alta" platform for the hindcast 90120700. In all panels the continuous, dashed lines and the circles show the same time series as in the previous figures. Upper panel: dots show the sse at two neighboring grid points. Dash-dots show the linear simulation with wave-dependent z_0. Central panel: dots show the sse obtained by varying the air-sea temperature difference. Lower panel: dots show the sse obtained by varying the bottom friction drag coefficient.

Note, anyway, that the results obtained by the surge model, whose dynamics is completely different, also support the dependence of the ssr on the wave spectrum. The case 90112312 is the only exception which might suggest that the wave-dependent ssr overestimates the actual value for a young wind sea. Anyway, the weather pattern of this storm was rather complicated and the wind direction probably not well predicted.

Obviously, one might argue that the actual momentum transfer to the marine current results from the difference between wind stress and bottom friction, and that this second contribution might have been overestimated by the model. However, there is an independent validation on the bottom friction coefficient that derives from the tuning of a barotropic circulation model against tidal data. This tuning, carried out with a linear model, suggested a value for C_{b} lower than the one used in this study. Moreover, this linear surge model is not very sensitive to the value of C_{b} during Sirocco storms. The dotted lines in the lower panel of fig. 8 show the results of two simulations with a wind-dependent

ssr, where C_{b} was increased and decreased by a factor ten. This large variation produced only a change of a few centimeters in the sse and cannot be considered a major source of uncertainty in our conclusions.

The air-sea temperature difference, $T_{\mathrm{a}} - T_{\mathrm{w}}$, *i.e.* the air-sea stability conditions, is not important. During a Sirocco storm, at the beginning of winter, the water can be warmer than the air and the neutral stress used could be lower than the actual stress. The actual difference in temperature is $0\,^{\circ}\mathrm{C} < T_{\mathrm{a}} - T_{\mathrm{w}} < 5\,^{\circ}\mathrm{C}$, which implies, at the high wind speed regime of a Sirocco storm, a rather small increase of the surface stress. The dotted lines in the central panel of fig. 8 show the results obtained assuming stable conditions ($T_{\mathrm{a}} - T_{\mathrm{w}} = 5$) or unstable conditions ($T_{\mathrm{a}} - T_{\mathrm{w}} = -5$) and a wind-dependent roughness. The effect of the air-sea stability on the sea level is only a few centimeters, and it cannot compensate for the difference between results based on the wind-dependent roughness and observations.

The choice of the model output point is not particularly crucial and there is no relevant gain by interpolating the model results to the actual location of the "Acqua Alta" platform. In fact, in the simulation based on the wind-dependent roughness, no relevant variation is obtained by choosing two grid points one step apart from the platform location (the two time series are represented by the dotted lines in the upper panel of fig. 8).

A more relevant source of uncertainty is the model numerics. A not negligible reduction of the surge is obtained by eliminating the nonlinear terms in the model equation (dash-dotted line in the upper panel of fig. 8). This indicates that the adoption of a multilayer model, capable of representing the shear of the current, or the choice of a different grid might have a non-negligible impact on the computed sse. Anyway, the effect of the nonlinear terms is clearly smaller than the effect of the wave-dependent roughness, and we do not think that it can affect the conclusions of this study.

4. – Summary and conclusions

This study shows that relevant benefits in the prediction of the surge and wind wave fields in the Northern Adriatic Sea can be obtained by adopting the wave-dependent ssr computed by Janssen's formula. Our results suggest that, in the short fetch conditions that are typical of small semi-enclosed basins, in order to obtain the correct surge level and wave field, the ssr (and therefore C_{D} and τ) should be increased with respect to the values derived from open-sea measurement based on averages over various values of wave ages, but mostly old wind sea. The fact that the results of both the surge and the wave model, in spite of their completely different dynamics, support the same conclusion is a substantial argument in favour of the dependence of the ssr on the wave spectrum.

There are, of course, uncertainties on the correct wind fields. These uncertainties are not expected to be large. Previous studies (Buzzi *et al.*, 1994) have shown that the BOLAM surface wind has a root mean square error of about 2.5 m/s and a bias of 0.5 m/s with respect to the observations. The consequences of errors of such magnitude are generally smaller than the differences discussed in these simulations. In this study, only one wind observation has been used, but its location is very representative, and it shows no major error that could suggest a different interpretation of our results. In principle, the availability of scatterometer satellite data could offer clear information on the spatial structure of the wind field, but the very limited coverage of the Adriatic Sea has prevented till now an effective validation of the wind field during an extreme event.

However, the computation of the wave-dependent wind stress was not carried out consistently in this study, because it was computed using simultaneously the wave-dependent

momentum transfer coefficient C_{D} and the wind speed that BOLAM computed with the Charnock formula. This suggests that, in this study, the wave-dependent stress was overevaluated and therefore the difference between the two approaches overestimated. The consistent computation can be carried out with a coupled atmosphere-wave-surge model and a recently developed code is planned to be applied to a significative set of hindcast cases (Lionello *et al.*, 1997), in order to investigate whether such consistency is a practically important issue.

Finally, four cases cannot be considered a statistically reliable data set, and the conclusion of this study should be validated in a more extensive investigation capable of simulating the forecast carried out in an operational center.

In spite of these limitations, this study demonstrates the feasibility of validating the ssr by the joint use of surge and wave models, and that the validation supports the dependence of the ssr on the wave spectrum.

* * *

The study was supported by the UE-MAST II project ECAWOM and by the CNR of Italy. The authors are indebted to DR. L. CAVALERI, Consorzio Venezia Nuova, and Centro Previsione Maree for the data used in this study.

REFERENCES

BLUMBERG A. F. and MELLOR G. L., *A description of a 3-dimensional coastal ocean circulation model*, in *3-dim coastal ocean models*, edited by N. S. HEAPS, Vol. **4** (American Geophisical Union, Washington, DC), 1987, pp. 1-16.

BUZZI A., FANTINI M., MALGUZZI P. and NEROZZI F., *Validation of a limited area model in cases of Mediterranean cyclogenesis: surface fields and precipitation scores*, *Meteorol. Atmos. Phys.*, **53** (1994) 137-153.

CAVALERI L., BERTOTTI L. and LIONELLO P., *Shallow water application of the third generation wave model WAM*, *J. Geophys. Res. C*, **94** (1989) 8111-8124.

CHARNOCK H., *Wind stress on a water surface*, *Quart. J. R. Meteor. Soc.*, **81** (1955) 639-640.

DAVIES A. M. and LAWRENCE J., *Examining the influence of wind and wind wave turbulence on tidal currents, using a three-dimensional hydrodynamic model including wave-current interaction*, *J. Phys. Oceanogr.*, **24** (1994) 2441-2460.

DONELAN M. A., DOBSON F. W., SMITH S. D. and ANDERSON R. J., *On the dependence of sea surface roughness on wave development*, *J. Phys. Oceanogr.*, **23** (1993) 2143-2149.

JANSSEN P. A. E. M., *Wave induced stress and the drag of the air flow over sea waves*, *J. Phys. Oceanogr.*, **19** (1989) 745-754. **21** (1991) 1631-1642.

JANSSEN P. A. E. M., *The quasi-linear theory of WIND wave generation applied to wave forecasting*, *J. Phys. Oceanogr.*, **21** (1991) pp. 1631-1642.

KOMEN G., JANSSEN P. A. E. M., MAKIN V. and OOST W., *On the sea state dependence of the Charnock parameter*, *The Global Atmosphere and Ocean System*, **5** (1997) 367-388.

LARGE W. G. and POND S., *Open ocean momentum flux measurements in moderate to strong winds*, *J. Phys. Oceanogr.*, **11** (1981) 324-336.

LIONELLO P., MALGUZZI P. and BUZZI A., *On the coupling between the atmospheric circulation and the ocean wave field: an idealized case*, *J. Phys. Oceanogr.*, **28** (1998) 161-177.

MAKIN V. K., KUDRYAVTSEV V. N. and MASTENBROEK C., *Drag of the sea surface*, *Boundary-Layer Meteorol.*, **73** (1995) 159-182.

MASTENBROEK C., BERGERS C. J. and JANSSEN P. A. E. M., *The dynamical coupling of a wave model and a storm surge model through the atmospheric boundary layer*, *J. Phys. Oceanogr.*, **23** (1993) 1856-1866.

SIMONS T. J., *Verification of numerical models of Lake Ontario*, Part I, *Circulation in spring and early summer*, *J. Phys. Oceanogr.*, **4** (1974) 507-523.

WAMDI GROUP (HASSELMANN S., HASSELMANN K., BAUER E., JANSSEN P. A. E. M., KOMEN G., BERTOTTI L., LIONELLO P., GUILLAUME A., CARDONE V. C., GREENWOOD J. A., REISTAD M., ZAMBRESKY L. and EWING J. A.), *The WAM model - A third generation ocean wave prediction model*, *J. Phys. Oceanogr.*, **18** (1988) 1776-1810.

WU J., *Wind-stress coefficient over sea surface from breeze to hurricane*, *J. Geophys. Res.*, **87** (1982) 9704-9706.